



The effect of Different Heavy Metals Pollutants in Refinery Effluent on Corrosion Rate of Carbon Steel

Ola M. Abdulwaheed¹, Basim O. Hasan¹, Sahir M Alzurajji^{2*}

Authors affiliations:

1) Department of Chemical Engineering, University of Al-Nahrain, Baghdad-Iraq.
ola.m.abduolwaheed@ced.nahrainuniv.edu.iq

2*) Department of Chemical Engineering, University of Al-Nahrain, Baghdad-Iraq.
basim.o.hasan@nahrainuniv.edu.iq

2*) HUN-REN Centre For Energy Research. Budapest-Hungary.
sahir.mohammed.alzurajji@ekcer.hu

Paper History:

Received: 9th Aug. 2023

Revised: 9th Aug. 2023

Accepted: 24th Nov. 2023

Abstract

The presence of heavy metal pollutants in refinery effluent significantly impacts the corrosion rate of carbon steel. The focus of this research is to analyze the impact of various inorganic pollutants, including copper, vanadium, nickel, and chromium ions, on the corrosion of carbon steel across different solutions. After conducting a thorough examination of various operating conditions, including pollutant concentration (ranging from 300-3000 ppm), temperature (30-60° C), and flow velocity (0-800 rpm). Our research shows that copper ions have the highest corrosion rate, with vanadium ions being a close second. Conversely, nickel and chromium had the most negligible impact on corrosion rate and, in some instances, even exhibited corrosion inhibition effects. It was also observed that an increase in flow velocity and temperature significantly amplified the corrosion rate of the metal ions investigated.

Keywords: Corrosion Rate, Carbon Steel, Inorganic Pollutants, Flow Velocity, Wastewater.

تأثير الملوثات المعدنية الثقيلة المختلفة في مياه الصرف الصحي على معدل تآكل الفولاذ الكربوني

علا محمود عبدالواحد، باسم عبید حسن، ساهر محمد الزرجي

المخالصة:

يؤثر وجود الملوثات المعدنية الثقيلة في النفايات السائلة من المصافي بشكل كبير على معدل تآكل الفولاذ الكربوني. يركز هذا البحث على تحليل تأثير الملوثات غير العضوية المختلفة، بما في ذلك أيونات النحاس والفاناديوم والنيكل والكروم، على تآكل الفولاذ الكربوني عبر محاليل مختلفة. بعد إجراء فحص شامل لظروف التشغيل المختلفة، بما في ذلك تركيز الملوثات (يتراوح من 300-3000 جزء في المليون)، ودرجة الحرارة (30-60 درجة مئوية)، وسرعة التدفق (0-800 دورة في الدقيقة). يظهر بحثنا أن أيونات النحاس لديها أعلى معدل للتآكل، وتأتي أيونات الفاناديوم في المرتبة الثانية. وعلى العكس من ذلك، كان للنيكل والكروم تأثير ضئيل للغاية على معدل التآكل، وفي بعض الحالات، أظهرت تأثيرات تثبيط التآكل. ولوحظ أيضًا أن الزيادة في سرعة التدفق ودرجة الحرارة أدت إلى تضخيم معدل تآكل الأيونات المعدنية التي تم فحصها بشكل كبير.

1. Introduction

Petroleum refineries face a significant challenge in the form of corrosion. This issue has garnered widespread attention in recent years as the global economy continues to rely heavily on industries that depend on oil and natural gas[1]. The petroleum industry involves a range of environments that can be corrosive, including some that are specific to this

industry [1,2]. However, the concentration and type of pollutants present in water depend on the plant configuration, operation procedures, and oil processing [3]. During petroleum processing, significant amounts of water are used in various stages, including desalting, distillation, thermal cracking, and catalytic cracking. This results in the generation of a substantial amount of wastewater.



Industrial wastewater from petroleum often has varying concentrations of organic and inorganic substances, including heavy metals, oils, grease, and various salts[4]. Water pollution harms humans and metallic equipment, such as pipelines, storage tanks, pumps, and heat exchangers, by causing corrosion attacks[5]. Industrial wastewater can cause water pollution through corrosion, as it can result in the presence of dissolved metal ions like Cu^{++} , Cd^{++} , and Pb^{++} . [6,7].

In addition, the wastewater contains a significant quantity of aromatic organic compounds, including polyaromatic hydrocarbons and phenolic substances. These substances are challenging to degrade naturally and pose a severe environmental risk [8]. The presence of some kinds of pollutants in the water or liquids with which industrial equipment deals can cause an appreciable corrosion rate, which is influenced by the pollutant's chemical and physical properties and operating conditions such as temperature and flow rate [6]. The presence of pollutants in wastewater can lead to significant corrosion damage to structures, mainly when they accumulate in some regions of process equipment or when left in tanks for an extended period. Based on the previous information, it is evident that various compounds generated by the petroleum industry, particularly during refinery processes, may significantly impact the corrosion tendencies of equipment. Therefore, exploring and evaluating these compounds from a corrosion perspective is essential. It is important to note that crude oil frequently comprises salt ions such as Cu, V, Cr, Ni, and Cd that can dissolve in water, posing a significant risk of corrosion damage to processing equipment [9]. This study focuses on analyzing the corrosion rate of carbon steel in wastewater from petroleum refineries. The wastewater contains inorganic pollutants, including copper, vanadium, chromium, and nickel. The study will examine how different temperatures and flow conditions impact corrosion rates.

2. Experimental work

In Figure 1, you can see the setup that was used for the experiment. It involved a water bath to get varying solution temperatures and a mechanical stirrer from (Stuart, UK) which had a 2-bladed impeller (Rushton turbine) to control the rotational speed. A carbon steel sheet was cut and fixed to the specimen holder in the solution to expose the specimen to the corrosive environment. The dimensions of the specimen were 40mm x 40mm x 0.7mm. A saturated calomel electrode (SCE) was used to measure the corrosion potential. Distilled water that was distilled once and solutions with different concentrations of metal ions, such as Cu, Ni, V, and Cr, were examined for their corrosive properties. The study also investigated the impact of temperature on corrosion rates in various solutions by varying temperatures between 30 °C and 60 °C. Furthermore, the effect of flow velocity was examined by altering the rotational speed from 0 to 800 rpm, which corresponds to a range of Reynold numbers 0 to 33260 based on impeller diameter.

Before each test, we prepared the specimen by abrading it with grade numbers 120, 180, 220, 400, and 2000 glass emery papers, then cleaned it with a plastic brush and tap water. We then rinsed it with distilled water, dried it with clean cloths, and immersed it in 5% HCl containing organic inhibitor (hexamine) for 30 seconds. After that, the specimen was rewashed with distilled water and immersed in ethanol for 2 minutes. We then placed it in an electric oven at approximately 90 °C for 5 minutes to dry and kept it in a vacuum desiccator with high-activity silica gel until use. Using a digital balance, the specimen was then weighted (w_1) to determine weight loss. After that, one face of the rectangular coupon was exposed to a corrosion environment, while the other face was completely insulated by insulating tape. Upon completion of the corrosion test, the corrosion products on the surface were cleaned using a plastic brush, then rinsing the specimen with tap water, brushing it with distilled water, and drying it with clean tissue. It was then kept in an electric oven at a temperature of 90 °C for 5 minutes for further drying and then weighed (w_2). As a result, the corrosion rate may be calculated as follows:

$$\text{CR (gmd)} = W/At \quad (1)$$

Where CR is the corrosion rate measured in gmd (gram/m².day), $W = w_1 - w_2$, A is the specimen area, and t is the exposure time. Table 1 presents the experimentally measured pH and electrical conductivity values for various solutions.

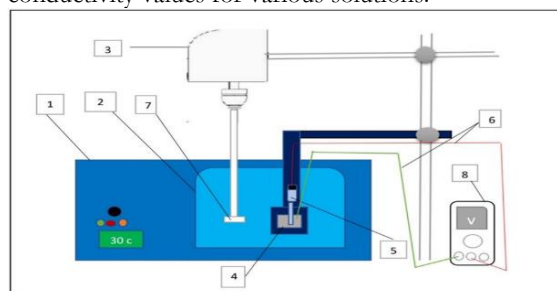


Figure (1): Experimental setup for weight loss experiments. 1-water bath, 2-beaker 2L, 3- agitators, 4-carbon steel, 5-reference electrode (SCE), 6 electrical connection wires, 7-glass impeller, 8- voltmeter.

Table (1): Measured pH and conductivity for different solutions

Components	Concentration of pollutant, ppm	pH	Conductivity, $\mu\text{s/cm}$
Distilled water	-----	7	0
CuCl ₂ .2H ₂ O	300	6.1	320
	700	5.3	920
	1000	4.8	920
	1500	4.6	1300
	2000	4.5	1680
	2500	5	2000
CrO ₃	1000	2.1	2290
VOSO ₄	1000	4.6	500
	2000	3.9	800
	300	6.6	240
NiCl ₂	1000	6.6	720
	2000	6.6	1400
	3000	7.1	1830
	3000	7.1	1830



3. Results and discussions:

3.1 Corrosion Potential

In Figure 2, the change in free corrosion potential versus the time is displayed for carbon steel in two different concentrations of $\text{CuCl}_2 \cdot 2\text{H}_2\text{O}$ solution (1000 and 2500 ppm) at 30°C and compared to distilled water. It is evident that the addition of copper ions causes the potential to shift to a more negative value. This observation aligns with findings from Mobin et al. [10] regarding metal ions. In the beginning, the potential decreases sharply with time to more negative due to the continuous corrosion. and forming a fouling layer consisting of iron oxide [11,12] and copper chloride. Then, the potential becomes almost constant with time. When in a steady state, the concentration of copper ions with higher values results in a more positive potential than those with lower concentrations. This means a higher concentration of Cu ions will shift the potential towards positivity. As shown in Fig. 2, it is noticeable that the potential in copper chloride solution is more positive than in distilled water at the beginning of the corrosion interval. This suggests that the presence of copper shifts the potential towards positivity, which can affect the corrosion rate.

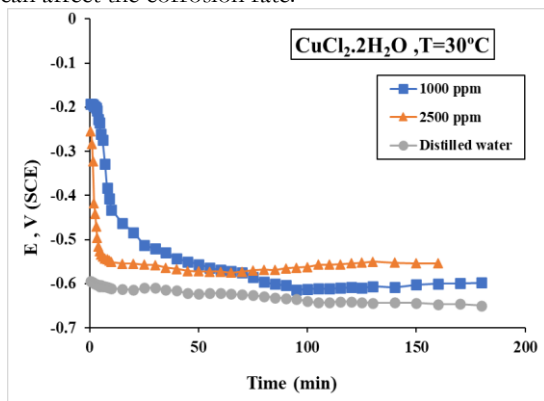


Figure (2): Variation of corrosion potential vs. time for $\text{CuCl}_2 \cdot 2\text{H}_2\text{O}$ solution at different concentrations

Figures 3 and 4 display the corrosion potential of CS vs. the time at different temperatures under stationary conditions with 1000 ppm $\text{CuCl}_2 \cdot 2\text{H}_2\text{O}$ and NiCl_2 , respectively. It is crucial to note that the corrosion potential shifts towards a more negative value as the temperature increases. This is a direct result of the decrease in oxygen concentration caused by the rise in temperature [13,14].

In $\text{CuCl}_2 \cdot 2\text{H}_2\text{O}$ solution at 30°C , Fig.5 displays the corrosion potential of CS versus the time for various agitation speeds. As the velocity increases, the potential shifts to more positive values because of the increased transport of Cu ions and O_2 from the solution bulk to the surface[15,16]. It is imperative to note that when dealing with $\text{CuCl}_2 \cdot 2\text{H}_2\text{O}$ solutions, the potential of CS is considerably higher than that of VOSO_4 and NiCl_2 solutions. This is due to the presence of copper ions, which inevitably causes the potential to shift positively.

The corrosion potential of Vanadium and Nickel solutions is barely influenced by velocity and lacks consistency, as illustrated in Figures 6 and 7. This implies that these ions have a negligible impact on

increasing corrosion potential. The fluctuation in corrosion potential with flow velocity is due to complicated phenomena arising from forming a coating layer on the metal surface. This layer restricts the amount of dissolved oxygen that can access the surface of the CS [17], as shown in Fig 8.

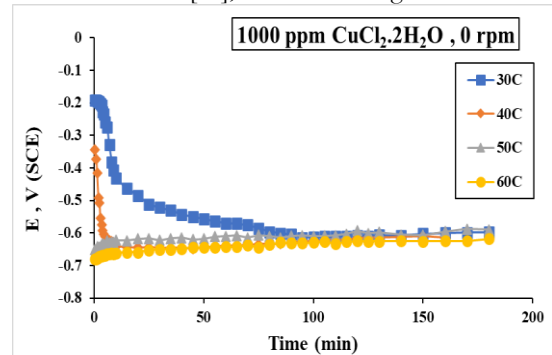


Figure (3): Variation of Corrosion potential vs. time at different temperatures for $\text{CuCl}_2 \cdot 2\text{H}_2\text{O}$ solution.

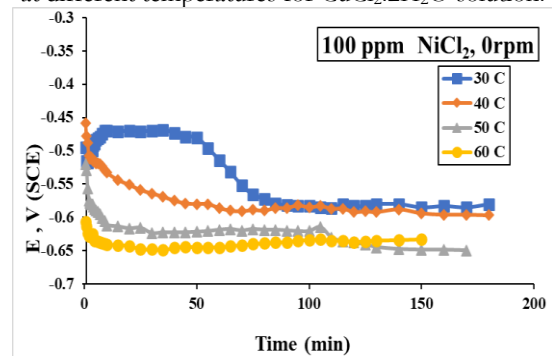


Figure (4): Variation of Corrosion potential vs. time at different temperatures for NiCl_2 solution.

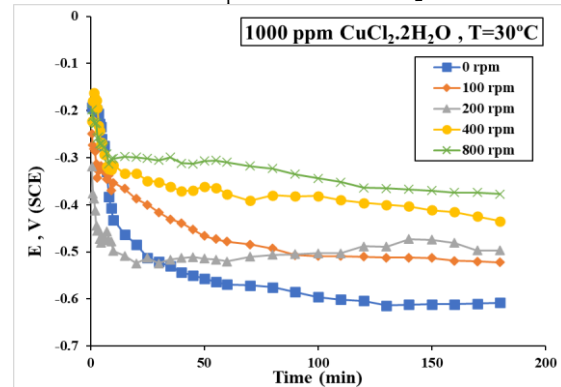


Figure (5): Corrosion potential vs. time with time for $\text{CuCl}_2 \cdot 2\text{H}_2\text{O}$ solution at different agitation velocity.

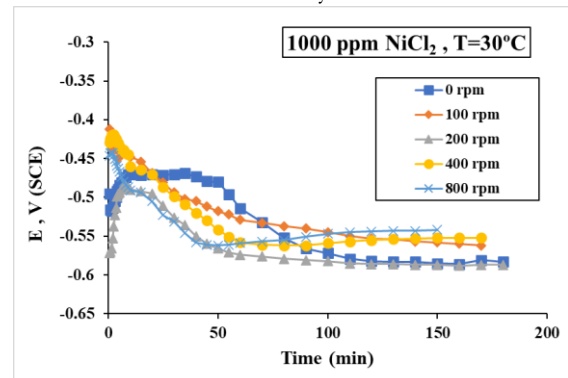


Figure (6): Corrosion potential vs. time with time for NiCl_2 solution at different agitation velocities.

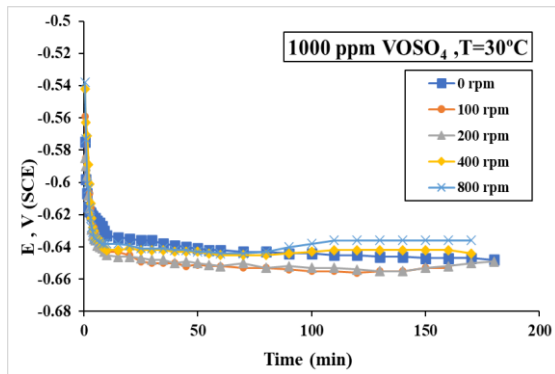


Figure (7): Corrosion potential vs. time with time for VOSO₄ solution at different agitation velocities.

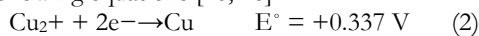


Figure (8): The pictures camera photos of carbon steel (a. before corrosion b. after 3h in NiCl₂ at 30°C)

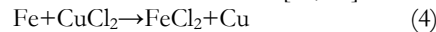
3.2 Corrosion rate (CR)

In Figure 9, the correlation between the concentration of pollutants expressed in gmd and the corrosion rate (CR) of CS is displayed. It is evident that the CR significantly increases as the concentration of CuCl₂.2H₂O increases. However, for other solutions, the increase in CR is minimal.

The reason for the high corrosion rate is due to the high potentials caused by the presence of copper ions, as demonstrated in Fig. 2. As iron metal is more electronegative than copper metal, it is oxidized as a Fe²⁺ ion. In contrast, the Cu²⁺ ion present in the solution is reduced as Cu-metal. The standard reduction potential of copper and iron are shown in the following equations [16, 18]



Since copper's reduction potential is more than Iron's, Copper will be reduced, and iron metal will be oxidized. The overall reaction is [16, 19]



As the concentration of CuCl₂.2H₂O increases, more copper will be displaced from copper sulfate by iron from carbon steel. This can result in a considerable loss in the weight of carbon steel, leading to an increase in corrosion rate. Additionally, higher concentrations of CuCl₂.2H₂O lead to an increase in the solution's electrical conductivity, as shown in Table 1. This increased electrical conductivity enhances the anodic and cathodic reactions, causing an increase in the corrosion rate. Figure 9 demonstrates that the corrosion rate caused by NiCl₂ also increases at high concentrations.

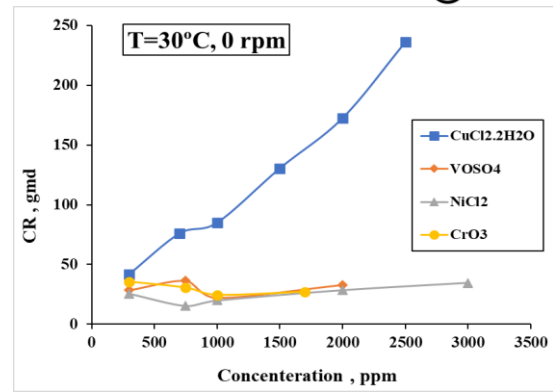


Figure (9): Variation of corrosion rate with CuCl₂.2H₂O, VOSO₄, NiCl₂, and CrO₃ concentration.

Figure 10 demonstrates how temperature affects the corrosion rate of carbon steel in the presence of 1000 ppm CuCl₂.2H₂O, VOSO₄, NiCl₂, and CrO₃, compared to distilled water in a stationary state. The graph conclusively shows that CuCl₂.2H₂O and VOSO₄ solutions experience a significant increase in corrosion rate with increasing temperature. This can be directly attributed to higher temperatures leading to increased O₂ diffusivity, which in turn enhances corrosion. It is also worth noting that the rate of almost all electro-chemical reactions increases as temperature rises. [20] When the temperature increases, the oxidation of iron is increased. This happens for two main reasons. Firstly, as the temperature increases, the diffusion coefficient of oxygen also increases, which promotes corrosion. Secondly, as the temperature increases, the solubility of oxygen decreases, which slows down the corrosion process [20, 21, 22]. The dissolution of CuCl₂.2H₂O results in elevated levels of chlorine and copper ions, whereas the dissolution of VOSO₄ raises the concentration of vanadium and sulfur ions. It is imperative to note that this can significantly expedite the corrosion rate. It can be seen in Fig. 10, it is evident that there is a significant reduction in CR for Ni and Cr ions. This decline indicates that these ions create a layer of coating on the metal surface, which prevents O₂ from reaching the metal surface.

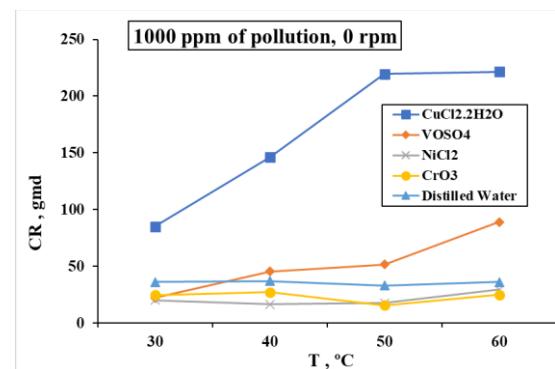


Figure (10): Variation of corrosion rate with temperature for CuCl₂.2H₂O, VOSO₄, NiCl₂, and CrO₃ solution.

In Figure 11, data is presented on the effect of agitation velocity on the corrosion rate of carbon steel in various solutions, including a 1000 ppm



$\text{CuCl}_2 \cdot 2\text{H}_2\text{O}$ solution. The results show that in the $\text{CuCl}_2 \cdot 2\text{H}_2\text{O}$ solution, as the agitation velocity increases from 0 to 800 rpm, the corrosion rate significantly increases from 128 to 2375.6 gmd (a 17.5-fold increase). In contrast, the vanadium solution shows a noticeable but less extreme increase of only about 2.7 times. Based on the analysis presented in Figure 11, it appears that the inclusion of NiCl_2 does not influence the rate of corrosion caused by flow velocity. However, it is apparent that an increase in velocity leads to a higher level of exposure of the steel surface to oxygen and metallic ions, accelerating the corrosion process [16, 25]. As the agitation velocity rises, the corrosion product layer begins to disintegrate partially, causing accumulation at the bottom of the beaker, as shown in Fig. 12. This exposes the surface to the solution again, leading to further corrosion through oxidation and reduction reactions. Figure 13 shows the camera and microscopic images of the specimen before and after corrosion for different flow velocities. It is evident that a higher flow velocity results in the formation of a corrosion product layer on the surface. The microscopic image for the highest speed, 800 rpm (image h) indicates high surface damage due to the high corrosive effect flow velocity.

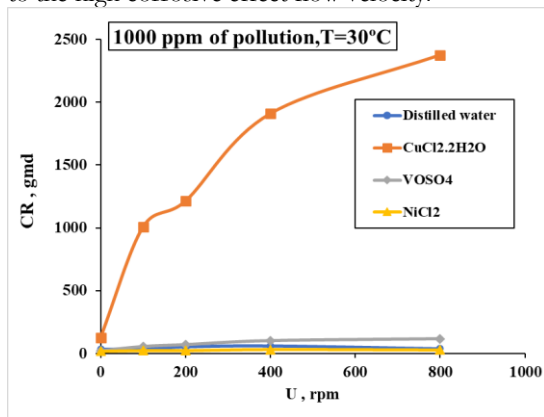


Figure (11): Variation of free corrosion rate with agitation velocity for distilled water, $\text{CuCl}_2 \cdot 2\text{H}_2\text{O}$, VOSO_4 , and NiCl_2 solution.



Figure (12): Beaker bottom at the end of the experiment at 30 °C and 1000 ppm $\text{CuCl}_2 \cdot 2\text{H}_2\text{O}$, for 100 rpm.

According to Li et al [24], the medium's flow affects induced corrosion in two ways: through mass transfer and surface shear stress. The speed at which the fluid flows plays a crucial role in erosion and directly influences the corrosion mechanism caused by flow. High fluid velocity increases wall shear stress, which can rupture passive films and expose fresh metal to corrosive media, increasing the corrosion rate. [23, 24] conducted a study on the results. The corrosion product layer sometimes becomes very thick, which is visible through visual observation. Figure 13 shows the removal and separation of this layer, where it drops on the beaker bottom under high corrosion rate conditions.

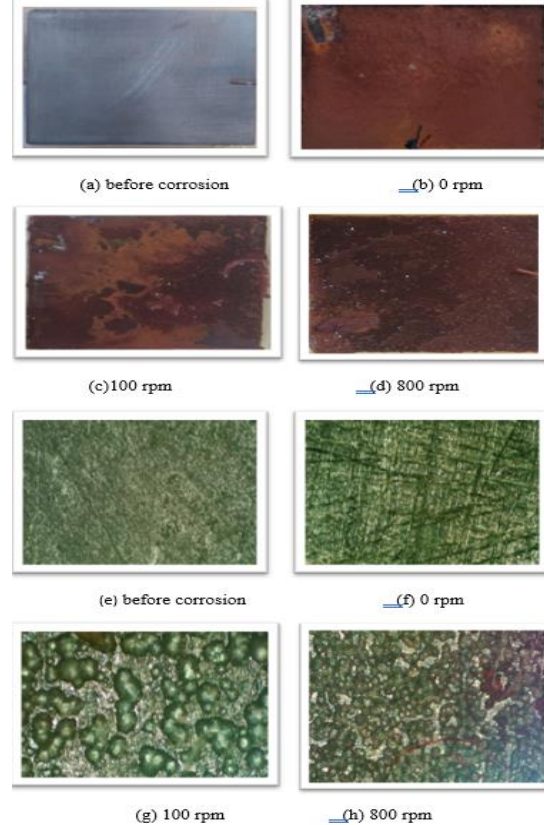


Figure (13): The pictures (a, b, c, and d) are camera photos of carbon steel in $\text{CuCl}_2 \cdot 2\text{H}_2\text{O}$ at 30 °C. While (e, f, g, and h) are microscope images of the same item.

4. Conclusions

After conducting thorough research, the following conclusions are drawn:

1. The corrosion rate of carbon steel increases when the concentration of $\text{CuCl}_2 \cdot 2\text{H}_2\text{O}$ solution is increased from 300 to 2500 ppm. This leads to 4.6 times increase in corrosion rate at 30°C and stationary conditions.

2. Increasing the temperature from 30 to 60 °C in stationary conditions for $\text{CuCl}_2 \cdot 2\text{H}_2\text{O}$ solution, the the corrosion rate increases by 0.7 times.

3. The corrosion rate of carbon steel increases when the stirring speed is increased from 0 rpm to 800 rpm in $\text{CuCl}_2 \cdot 2\text{H}_2\text{O}$ solution. This leads to a 17.5 times increase in corrosion rate.

4. The corrosion rate of carbon steel in VOSO_4 solution is slight at 30°C. It increases by 2.7 times with a temperature increase from 30 to 60°C. The



corrosion rate slightly increases with increasing stirring speed from 0 to 800 rpm.

5. The corrosion rate in NiCl_2 and CrO_3 solutions is generally low, even at high concentrations, temperatures, and speeds.

6. The corrosion potential in $\text{CuCl}_2 \cdot 2\text{H}_2\text{O}$ solution decreases sharply to a more negative value and then becomes nearly constant over time.

7. In $\text{CuCl}_2 \cdot 2\text{H}_2\text{O}$ and NiCl_2 solutions with a temperature range of 30-60°C, the potential for corrosion is shifted to more negative values. It is noticed that there is a corrosion inhibition effect of the accumulated layer of NiCl_2 on the carbon steel surface.

8. With increased speed and concentration of copper ions, the corrosion potential tends to be more positive. While it tends to be more negative with increasing temperature.

7. References:

- [1] Al-Moubaraki, A. H., & Obot, I. B. (2021). Corrosion challenges in petroleum refinery operations: Sources, mechanisms, mitigation, and future outlook. *Journal of Saudi Chemical Society*, 25(12), 101370.
- [2] Mizzouri, N. S., & Shaaban, M. G. (2013). Individual and combined effects of organic, toxic, and hydraulic shocks on sequencing batch reactor in treating petroleum refinery wastewater. *Journal of hazardous materials*, 250, 333-344.
- [3] Saïen, J., & Nejati, H. (2007). Enhanced photocatalytic degradation of pollutants in petroleum refinery wastewater under mild conditions. *Journal of hazardous materials*, 148(1-2), 491-495.
- [4] El-Shamy, A. M., El-Boraey, H. A., & El-Awdan, H. F. (2017). Chemical treatment of petroleum wastewater and its effect on the corrosion behavior of steel pipelines in sewage networks. *J Chem Eng Process Technol*, 8(1).
- [5] Woodard, F.. *Industrial waste treatment handbook*. 1st Edition, USA, Library of Congress Cataloging-in Publication Data Elsevier, 2001.
- [6] Sapkota, K. R. (2013). Effect of corrosive pollutants on Gram Production. *Janapriya Journal of Interdisciplinary Studies*, 2, 61-64.
- [7] Lusinier, N., Seyssiecq, I., Sambusiti, C., Jacob, M., Lesage, N., & Roche, N. (2021). A comparative study of conventional activated sludge and fixed bed hybrid biological reactor for oilfield produced water treatment: Influence of hydraulic retention time. *Chemical Engineering Journal*, 420, 127611.
- [8] Al-Khalid, T., & El-Naas, M. H. (2018). Organic contaminants in refinery wastewater: characterization and novel approaches for biotreatment. *Recent insights in petroleum science and engineering*, 371.
- [9] Nosier, S. A. (2003). The effects of petroleum refinery wastewater on the rate of corrosion of steel equipment. *Anti-Corrosion Methods and Materials*, 50(3), 217-222.
- [10] Mobin, M., Malik, A. U., Andijani, I. N. (2007). The effect of heavy metal ions on the localized corrosion behavior of steels. *Desalination*, 217(1-3), 233-241.
- [11] Sherif, E. S. M. (2014). A comparative study on the electrochemical corrosion behavior of iron and X-65 steel in 4.0 wt% sodium chloride solution after different exposure intervals. *Molecules*, 19(7), 9962-9974.
- [12] Slaimana, Q. J., & Hasan, B. O. (2010). Study on corrosion rate of carbon steel pipe under turbulent flow conditions. *The Canadian Journal of Chemical Engineering*, 88(6), 1114-1120.
- [13] Hasan, B. O. (2015). Galvanic corrosion of aluminum-steel under two-phase flow dispersion conditions of CO_2 gas in CaCO_3 solution. *Journal of Petroleum Science and Engineering*, 133, 76-84.
- [14] Hasan, B. O., & Aziz, S. M. (2017). Corrosion of carbon steel in two phase flow (CO_2 gas- CaCO_3 solution) controlled by sacrificial anode. *Journal of Natural Gas Science and Engineering*, 46, 71-79.
- [15] Mahato, B. K., Cha, C. Y., & Shemilt, L. W. (1980). Unsteady state mass transfer coefficients controlling steel pipe corrosion under isothermal flow conditions. *Corrosion Science*, 20(3), 421-441.
- [16] Ali, Marwa Essam Mohammed. "Corrosion behavior of carbon steel in the presence of different corrosive pollutants under concentration cell formation." MSC thesis, Department of Chemical Eng., Al-Nahrain University, 2019.
- [17] Marcus, P. *Corrosion mechanisms in theory and practice*. CRC press, 2001.
- [18] Perez N. "Electrochemistry and Corrosion Science". Kluwer Academic Publishers, USA, 2004.
- [19] Verma, N. K., & Verma, N.. *Academic Chemistry IX*. Laxmi Publications, (2012).
- [20] Revie, R. W. . *Corrosion and corrosion control: an introduction to corrosion science and engineering*. John Wiley & Sons, 2008.
- [21] Hasan, B. O., & Sadek, S. A. (2013). Corrosion behavior of carbon steel in oxygenated sodium sulphate solution under different operating conditions. *Adv. Chem. Eng. Res*, 2(3), 61-71.
- [22] Roberge, P. R. . *Handbook of corrosion engineering*. New York: Mcgraw-hill, 2000.
- [23] Yong, X. Y., Zhang, Y. Q., Li, D. L., Ji, J., Qu, Y. X., & Wang, J. D. (2011). Effect of near-wall hydrodynamic parameters on flow induced corrosion. *Corrosion Science and Protection Technology*, 12(3), 245-250.
- [24] Li, Z., Zhang, J., & Cheng, J. (2017). The influence of critical flow velocity on corrosion of stainless steel. *Journal of Failure Analysis and Prevention*, 17, 1234-1240.
- [25] Shreir, L. L., Jarman, R. A., Burstein, G. T. 2000. "Corrosion: Metal". *Environment Reactions*, vol. 1, New Yourk, 2000.